Electronic structure and optical properties of concentric-shell fullerenes from electron energy-loss spectroscopy in transmission

Pichler, T.; Knupfer, M.; Golden, M.S.; Fink, J.; Cabioc'h, T.

[Link to publication](#)

Electronic structure and optical properties of concentric-shell fullerenes from electron-energy-loss spectroscopy in transmission

T. Pichler

Institut für Materialphysik Universität Wien, A-1090 Wien, Austria

M. Knupfer, M. S. Golden, and J. Fink

Institute for Solid State and Materials Research (IFW) Dresden, P.O. Box 270016, D-01171 Dresden, Germany

T. Cabioc'h

Université de Poitiers, Laboratoire de Métallurgie Physique, UMR 6630 CNRS, Bâtiment SP2MI, Teleport 2, Bd 3, BP 179, 86660 Futuroscope Cedex, France

We present momentum-dependent measurements of the loss function of bulk samples of concentric-shell fullerenes using electron-energy-loss spectroscopy in transmission. It is shown that the π and $\pi + \sigma$ plasmons of these so-called carbon onions exhibit a significant momentum dependence, with a dispersion coefficient of about two-thirds of that of the corresponding plasmons in graphite. The optical properties derived from a Kramers-Kronig analysis are reminiscent of those found for polycrystalline disordered graphite. Furthermore, we find no changes of the electronic properties by alternating the average diameter of these carbon nanoparticles between 4 and 8 nm. Consequently, concentric-shell fullerenes can be regarded as spherical graphitic nanoparticles, whose electronic structure and optical properties, down to a particle size of at least 4 nm, are strongly governed by the band structure of graphite.

PACS number(s): 61.48.+c, 73.21.−b, 71.20.Tx, 78.20.Ci

I. INTRODUCTION

In 1992 Ugarte discovered concentric shell carbon clusters after intense electron irradiation of carbon soot in a transmission electron microscope (TEM).[1] These so-called ''carbon onions'' consist of concentric spherical layers of carbon with an interlayer distance of 0.34 nm, which is close to that of graphite. TEM has also been used to demonstrate an interesting application of these nanostructures as nanoscopic pressure cells which can be used to produce nanodiamond in their core.[2] Although further production techniques of concentric-shell fullerenes, like annealing of diamond nanoparticles[3] or carbon black,[4] or high-dose carbon ion implantation into silver substrates held at elevated temperature,[5] have been developed, most of the work on the solid-state physics and chemistry of these systems has been hindered by the low production rate and reproducibility, as well as the broad size distribution of the produced carbon nanostructures. Only the ion implantation method has been shown to have the main advantage to produce films of uniformly distribution of concentric-shell fullerenes with a narrow diameter distribution.[6] A narrow diameter distribution is needed to identify the intrinsic physical properties of bulk samples of these concentric-shell carbon nanostructures. Recently, Fourier transform infrared spectroscopy was used to characterize such carbon nanostructures produced by ion implantation.[7] From an analysis of the infrared allowed vibrations, it was shown that these carbon nanostructures consist of concentric spheres of fullerenes C_n ($n=60, 240, \dots$) in agreement with the proposed structure.[8] The electronic properties of such carbon onions were characterized by spatially resolved electron energy-loss spectroscopy (EELS) in transmission[5,9,10] and by EELS in reflection.[11] From a comparison of the plasmon positions in transmission EELS and

in reflection EELS at different geometries and electron beam energies, additional features were observed in the loss function, and were explained by tangential and radial surface plasmons. In addition simulations using a generalized model based on nonrelativistic local dielectric response theory were used to simulate spatially resolved EELS measurements of individual shells. A good agreement was observed, taking into account the anisotropy of the electronic properties via the frequency dependent dielectric tensor of graphite.[9,12]

In this paper we present momentum-dependent EELS in transmission of concentric-shell fullerenes which have been produced by ion implantation and which have a uniform diameter distribution. These measurements are conducted in a purpose-built machine with a high- energy and -momentum resolution but with no spatial resolution, and are therefore complementary to the spatially resolved EELS measurements reported previously. Our results are compared to those from C_{60}, as an example of single-shell fullerenes, and to graphite. We show that the π and $\pi + \sigma$ plasmons in these systems exhibit a finite dispersion, in contrast to single-shell fullerenes. Furthermore, we present the optical properties of those films of concentric-shell fullerenes, which have been derived performing a Kramers-Kronig analysis (KKA). Our results show that concentric shell fullerenes are intermediate between fullerenes and graphite, and support their description as spherical graphitic nanostructures.

II. EXPERIMENT

Three different batches of carbon onions (which had mean diameters of 4, 5, and 8 nm, respectively) were synthesized by implantation of carbon ions with 120 keV (doses: 5×10^{16}, 1×10^{17}, and $3 \times 10^{17}/cm^{-2}$) at 500 °C into thin silver films that were deposited onto fused silica substrates.
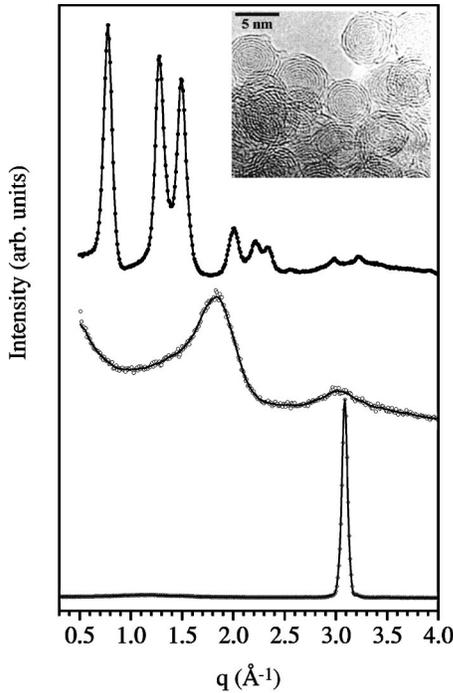
FIG. 1. Electron diffraction profiles of C_{60} (●), concentric-shell fullerenes (○), and graphite in the (100) direction (◇). The inset to the figure shows a typical TEM image of the investigated concentric shell fullerenes.

FIG. 2. C $1s$ core excitation spectra of concentric-shell fullerenes (○), graphite (momentum transfer parallel to the (001) direction (◇), and C_{60} (●).

These concentric-shell fullerenes studied here are identical to those previously studied in Ref. 13. In order to produce free-standing films for the EELS experiments, the silver was evaporated by annealing the sample in high vacuum for 10 h at 850°C, and the exposed onions were then transferred with an effective film thickness of about 1000 Å onto standard copper electron microscopy grids.

EELS in transmission was carried out in a purpose-built high-resolution spectrometer[14] which combines both good energy *and* momentum resolution. For the data shown here, energy and momentum resolutions of 160 meV and 0.06 Å^{-1} (valence-band excitations) and of 340 meV and 0.12 Å^{-1} (core-level excitations) were chosen. All spectra were recorded at room temperature.

III. RESULTS AND DISCUSSION

A first characterization of the samples was performed by measuring the electron-diffraction profiles. Figure 1 shows typical electron-diffraction profiles of concentric-shell fullerenes in comparison to those of graphite in the (100) direction and C_{60}. All studied films of concentric-shell fullerene showed electron diffraction patterns similar to that in Fig. 1, in particular no changes were observed as a function of their mean diameter. The inset to the figure shows a typical TEM image of the investigated concentric shell fullerenes. Two very broad diffraction features are observed at about 1.8 and 3 Å^{-1}. Whereas the latter can be assigned to a remainder of the ''in-plane'' graphite Bragg peaks, the peak at 1.8 Å^{-1} is related to the c axis (001) peak of graphite, and thus arises from the shell structure of these carbon
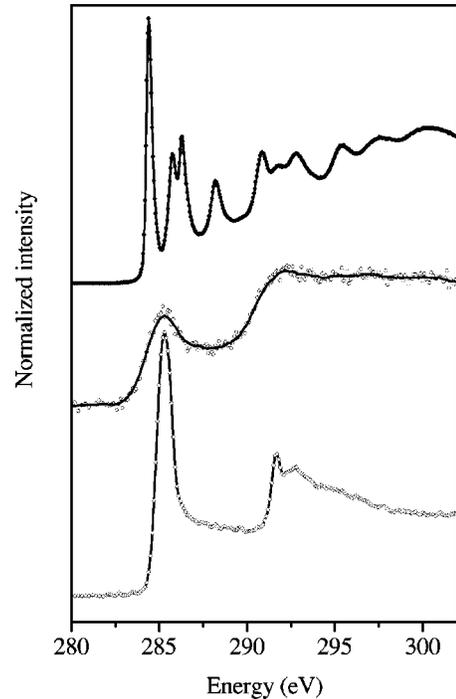
nanostructures. Generally, the concentric-shell fullerene films studied here have a diffraction pattern which is very similar to that of strongly disordered graphite.

In order to study the unoccupied electronic states and the dielectric response of concentric-shell fullerenes we have carried out measurements of the C $1s$ core-level excitations and the low-energy-loss function $Im(-1/\epsilon)$, respectively. Again, the response of the concentric-shell fullerenes was found to be independent of their mean diameter. Therefore, we only show representative spectra stemming from samples with a mean diameter of 5 nm.

In Fig. 2, the C $1s$ core-level excitation spectrum of such concentric-shell fullerenes is depicted in comparison to those of graphite and C_{60}. The spectrum of graphite shows the well-known $\pi^\star$ resonance at about 285 eV and a $\sigma^\star$ threshold at about 291 eV.[15] For C_{60} below the $\sigma^\star$ onset at about 290 eV, several structures appear, which can be assigned to excitations into the unoccupied $\pi^\star$-derived molecular states.[16] The core excitation spectra of the concentric-shell fullerenes show a broad resonance related to the $\pi^\star$-derived states at about 285.2 eV, and a $\sigma^\star$ threshold at 291 eV. The overall shape of the C $1s$ core-level excitation spectrum of these carbon nanostructures is very similar to that of a strongly broadened spectrum of graphite. Compared to C_{60}, no fine structure related to transitions into narrow molecular states is observed. This is a first indication that the electronic structure of the carbon concentric-shell fullerenes is essentially derived from the band structure of graphite. A comparison to directional-dependent C $1s$ excitation measurements[17,18] of graphite reveals that the C $1s$ spectrum of concentric-shell fullerenes is reminiscent of an iso-
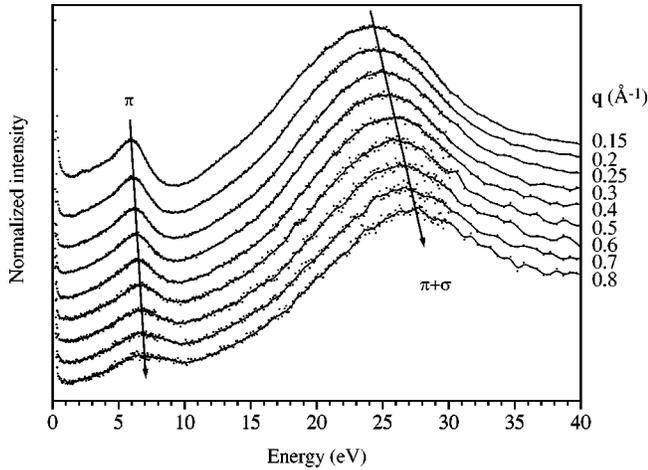
FIG. 3. The loss function of concentric-shell fullerenes from EELS in transmission as a function of q. The arrows indicate the dispersion of the π plasmon and the $\pi+\sigma$ plasmon.

FIG. 4. The dispersion of the π and $\pi+\sigma$ plasmons of concentric-shell fullerenes ($\bigcirc$) from EELS in transmission measurements. When invisible, the error bars are within the size of the symbols. For comparison the dispersion of the π and $\pi+\sigma$ plasmons in graphite for momentum transfers parallel to the planes ($\diamondsuit$) and C_{60} ($\bullet$) are depicted.

tropic average of the in-plane and out-of-plane graphite spectra. In graphite, the features at the $\pi^\star$ (Ref. 19) and $\sigma^\star$ (Ref. 18) onsets are both strongly excitonic in nature, and it is reasonable to assume that the same holds for the concentric-shell fullerenes.

The momentum-dependent optical properties can be derived from the energy-loss spectrum in the energy region of the valence excitations. In an EELS experiment, the features in the measured loss function are a direct probe of the collective excitations of the system under consideration. For energies below about 50 eV these features are related either to charge-carrier plasmons or interband or intraband excitations. On performing a Kramers-Kronig analysis the dielectric response function $[\epsilon(q,E)]$ and the optical conductivity can be derived. From the momentum dependence of the loss function, the degree of localization of the electronic excitations can be probed. Transitions between localized states give rise to a vanishingly small dispersion of the corresponding features in the loss function, as has been observed, for example, for the features related to the excitations between the molecular orbitals of C_{60}.[20] On the other hand, excitations between delocalized states generally exhibit a band-structure-dependent dispersion relation, as found for instance in the case of graphite.[21] In Fig. 3 the loss function of the concentric-shell fullerenes, measured as a function of the momentum transfer q, is depicted. The arrows indicate the position of the so-called π plasmon, which represents the collective excitation of the π-electron system, and the $\pi+\sigma$ plasmon (the collective excitation of all valence electrons) as a function of momentum transfer. The energy position of these plasmons at 6 and 24 eV for a momentum transfer of 0.15 Å^{-1} confirms theoretical predictions that the π-plasmon should occur in the energy range of 5–7 eV, and the $\pi+\sigma$ plasmon at about 25 eV in the EELS spectra of isolated concentric carbon shells.[22,12] Furthermore, our results are in good agreement with those from previously reported spatially resolved transmission EELS data, which were taken on similar samples but with lower energy and momentum resolution using a transmission electron
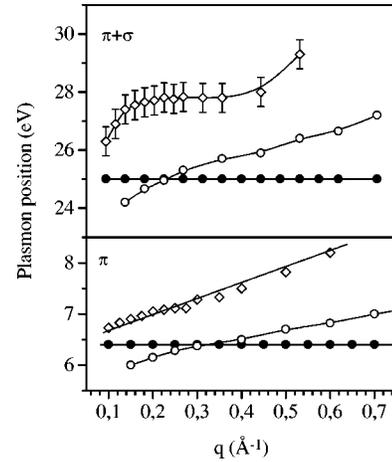
microscope.[5,9,10] Recent reflection EELS measurements on similar carbon concentric-shell fullerenes, which were conducted at different primary energies, revealed additional features at 13.5, 14.5, and 16.7 eV, which have been assigned to σ-$\pi^\star$ interband transitions, the surface radial plasmon σ-$\pi^\star$, and the surface tangential σ-$\sigma^\star$ plasmon.[11] However, the strong interaction with the silver substrate complicated the unambiguous identification of the π surface and volume plasmons in the highly surface sensitive high-resolution EELS experiments. In the transmission EELS measurements presented here, the total absence of silver in the samples, combined with the negligible surface scattering contribution to the measured loss function, even at low q,[23] means that one arrives at the true, representative volume dielectric properties of concentric-shell fullerenes.

As already mentioned above, the momentum dependence of the loss function also yields information about the degree of localization of the electronic states between which the excitations take place, as recently demonstrated for other carbon nanostructures like bundles of single-wall carbon nanotubes.[24] Figure 4 compares the energy position of the π and $\pi+\sigma$ plasmons of concentric-shell fullerenes, graphite (in plane), and C_{60} as a function of momentum transfer q. In small molecular nanostructures like C_{60}, the π and $\pi+\sigma$ plasmons exhibit a vanishingly small dispersion as they are related to interband transitions between localized molecular orbitals. In graphite, the dispersion of π and $\pi+\sigma$ plasmons, which are related to interband transitions at about 4.5, 13, and 15 eV, is directly correlated with the band structure of the graphene sheet.[21] For a semimetal-like graphite, a gap opens in the excitation spectrum at finite momentum transfer which leads to the observed dispersion of the plasmons. keeping these points in mind, the observed dispersion of the π and the $\pi+\sigma$ plasmons demonstrates the graphitic nature of these spherical carbon nanostructures with a significant delocalization of the π electrons. The observed plasmon dis-
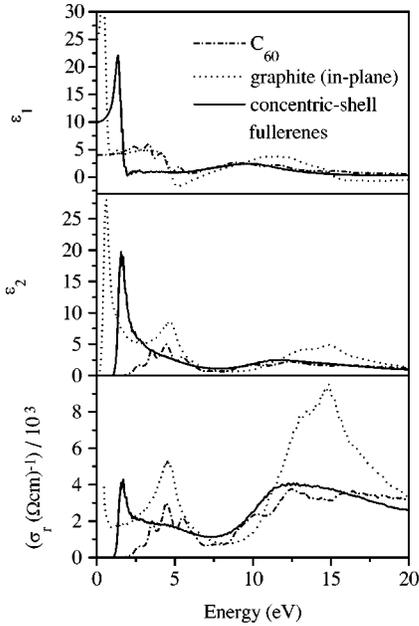
FIG. 5. The real and imaginary parts of the dielectric function (upper panels) and the real part of the optical conductivity (σ_r) at low momentum transfer ($q = 0.15$ Å^{-1}) for concentric-shell fullerenes (solid line) , C_{60} ($- \cdot -$), and graphite [polarized in plane ($\cdots$)].

persion is about two-thirds of that measured for graphite, with a momentum transfer parallel to the graphene sheets. The reduced plasmon dispersion compared to in-plane graphite can be explained by a reduced effective momentum transfer q_{eff} in the concentric-shell fullerenes. q_{eff} can be envisaged as an average of the projections of the momentum transfer q onto the carbon shells. As this projection is only parallel to the graphitic shells for two directions, q_{eff} is smaller than q in graphite parallel to the plane. Concentric-shell fullerenes can therefore be envisaged as spherical graphitic nanoparticles with a band structure which strongly related to that of graphite itself.[22]

The real (ϵ_1) and imaginary (ϵ_2) parts of the dielectric response function and the optical properties can be derived by a KKA of the measured loss function. The results of such a KKA are depicted in the upper panels of Fig. 5 for the concentric-shell fullerenes, C_{60}, and graphite (momentum transfer parallel to the graphene sheets). In the lowest panel the corresponding real part of the optical conductivity, $\sigma_r(E)$, is plotted, whereby $\sigma_r(E) = (E/\hbar)\epsilon_0\epsilon_2(E)$ is a measure of the joint electronic density of states. For the KKA the loss function was normalized to $\epsilon_r(0)$. For the concentric-shell fullerenes we have taken $\epsilon_r(0)$ to be 10 ($q = 0.15$ Å^{-1}), which corresponds to the dielectric constant of polycrystalline graphite at $q = 0.15$ Å^{-1} following the spherical average of the extrapolated values of in-plane graphite [Ref. 21 and out of plane graphite (Ref. 25)]. In general, the optical conductivity of these sp^2-conjugated car-

bon systems show peaks due to transitions between the (π/σ) and the ($\pi^\star/\sigma^\star$) electronic states. In C_{60} these peaks are very pronounced which is consistent with the high symmetry of the molecule and the weak van der Waals interactions in the solid state,[16] making C_{60} a prototypical zero-dimensional solid. In graphite three broad features are observed at 4.5 ± 0.05, 13 ± 0.05, and 15 ± 0.05 eV. Their breadth is an expression of the bandlike nature of the electronic states in the graphite plane. In addition, a strong peak occurs at the low energy end of the optical conductivity. At zero momentum transfer this peak would give rise to the charge-carrier plasmon in graphite; at finite momentum transfer it corresponds to the gap transition in the semimetal.[21] For the concentric-shell fullerenes we also find a strong peak at 1.7 eV and three broad features at energies slightly lower than those in graphite, i.e., at 4.4 ± 0.2, 12.2 ± 0.3, and 14.3 ± 0.3 eV. This furthermore underlines the similarity of concentric-shell fullerenes with diameters larger than 4 nm, and graphite as regards the electronic properties of these systems. In analogy to intercalated graphite compounds, one thus can also expect further interesting properties of concentric-shell fullerenes upon intercalation with *p*- or *n*-type dopants.

IV. CONCLUSION

In summary, we have demonstrated that momentum-dependent high-resolution EELS in transmission measurements of concentric-shell fullerenes with a narrow diameter distribution can provide insight into their electronic and optical properties. No change of the electronic properties of the carbon concentric-shell fullerenes is observed within the resolution of the measurements upon varying their mean diameter between 4 and 8 nm. From electron diffraction we find a similarity to strongly disordered polycrystalline graphite. The C $1s$ absorption spectra, which give a measure for the matrix element weighted unoccupied density of states, most closely resemble an average of the in-plane and out-of-plane graphite spectra, as one would expect for polycrystalline graphite. In contrast to single-shell fullerenes, a finite dispersion of the π and the $\pi + \sigma$ plasmons, which is about two-thirds of that in graphite, is observed. The optical conductivity shows electronic transitions at energy positions slightly lower than in graphite. Therefore, these concentric-shell fullerenes can be seen as a link inbetween fullerenes and graphite. Their electronic properties are strongly related to those of graphite, and they deserve the name spherical graphitic nanoparticles.

[1] D. Ugarte, Nature (London) **359**, 707 (1992).

[2] F. Banhart and P.M. Ajayan, Nature (London) **382**, 443 (1996).

[3] V.L. Kuznetsov, A.L. Chuvilin, Y.V. Butenko, I.Y. Malkov, and V.L. Titov, Chem. Phys. Lett. **222**, 343 (1994).

[4] D. Ugarte, Carbon **32**, 1245 (1994).

[5] T. Cabioc'h, J.C. Girard, M. Jaouen, and M.F. Denanot, Europhys. Lett. **38**, 471 (1997).

[6] T. Cabioc'h, M. Jaouen, M.F. Denanot, and P. Bechet, Appl. Phys. Lett. **73**, 3096 (1998).

[7] T. Cabioc'h, A. Kharbach, A. Le Roy, and J.P. Riviere, Chem. Phys. Lett. **285**, 216 (1998).

[8] K.G. McKay and H.W. Kroto, J. Chem. Soc., Faraday Trans. **88**, 2815 (1992).

[9] T. Stöckli, J.-M. Bonard, A. Chatelain, Z.L. Wang, and P. Stadelmann, Phys. Rev. B **61**, 5751 (2000).

[10] M. Kociak, L. Henrard, O. Stéphan, K. Suenaga, and C. Colliex, Phys. Rev. B **61**, 13 936 (2000).

[11] L. Henrard, F. Malengreau, P. Rudolf, K. Hevesi, R. Caudano, Ph. Lambin, and T. Cabioc'h, Phys. Rev. B **59**, 5832 (1999).

[12] T. Stöckli, J.M. Bonard, A. Chatelain, Z.L. Wang, and P. Stadelmann, Phys. Rev. B **57**, 15 599 (1998).

[13] T. Cabioc'h, E. Thune, and M. Jaouen, Chem. Phys. Lett. **320**, 202 (2000).

[14] J. Fink, Adv. Electron. Electron Phys. **75**, 121 (1989), and references therein.

[15] E.J. Mele, and J.J. Ritsko, Phys. Rev. Lett. **43**, 68 (1979).

[16] E. Sohmen and J. Fink, Phys. Rev. B **47**, 14 532 (1993).

[17] P.E. Batson, Phys. Rev. B **48**, 2608 (1993).

[18] Y. Ma, P. Skytt, N. Wassdahl, P. Glans, D.C. Mancini, J. Guo, and J. Nordgren, Phys. Rev. Lett. **71**, 3725 (1993).

[19] P.A. Brühwiler, A.J. Maxwell, C. Puglia, A. Nilsson, S. Andersson, and N. Martensson, Phys. Rev. Lett. **74**, 614 (1995).

[20] H. Romberg, E. Sohmen, M. Merkel, M. Knupfer, M. Alexander, M.S. Golden, P. Adelmann, T. Pietrus, J. Fink, R. Seemann, and R.L. Johnson, Synth. Met. **55-57**, 3038 (1993).

[21] K. Zeppenfeld, Z. Phys. **243**, 229 (1971).

[22] A.A. Lucas, L. Henrard, and Ph. Lambin, Phys. Rev. B **49**, 2888 (1994); L. Henrard, and Ph. Lambin, J. Phys. B **29**, 5127 (1996).

[23] For carbon nanostructures with a diameter of about 5 nm, no significant surface plasmon contribution is expected above about 0.02 Å^{-1}, much lower than the applied momentum transfer of 0.15 Å^{-1} of the EELS spectra that was used for the KKA.

[24] T. Pichler, M. Knupfer, M.S. Golden, J. Fink, A.G. Rinzler, and R.E. Smalley, Phys. Rev. Lett. **80**, 4729 (1998).

[25] H. Venghaus, Phys. Status Solidi **66**, 154 (1974).